NUMERICAL MODELLING OF WAVE OVERTOPPING AT EMERGENT AND OVERWASHED DYKES

Andrea N. Raosa[1], Barbara Zanuttigh[2], Javier L. Lara[3]

Abstract

The purpose of this contribution is the analysis of the characteristics of the flow (velocities and layer thicknesses) on the dike crest. This analysis is carried out on a numerical database derived by running the Rans-Vof code (IH-2VOF) developed by the University of Cantabria in presence of submerged impermeable structures characterized by different slopes. For zero freeboard structures, numerical flow depths and velocities over the dike crest are represented quite well by the theoretical existing models. In case of over-washed structures, the numerical discharges can be accurately reproduced by the sum of the overtopping and storm surge components.

Key words: real wave overtopping, numerical simulations, overwashed dykes, RANS-VOF model**.**

1. Introduction

The increase of frequency and intensity of storms, combined with the uncertainties related to extreme events and climate change, pose serious challenges in the long term design of defences from coastal flooding. Due to economic constraints, environmental and aesthetic impact, dikes cannot be as high as the climate conditions would require for full protection of the inland areas. Therefore it is more likely that in the next future many dikes will operate for longer times at lower crest freeboards, i.e. close to mean sea level or even overwashed. For design purposes, accurate estimates of the statistics of overtopping waves in terms of flow depths, duration and especially velocities for a set of climate conditions are needed and have to be combined with consolidated criteria for identifying tolerable overtopping threshold.
In literature it is possible to find some theories that describe flow depths and velocities over the dike crest for emerged conditions, for example the theoretical model by Schuttrumpf and Oumeraci (2005). For zero freeboard and submerged conditions, instead, a theoretical approach that allows to know the flow characteristics over the dike crest is not available.
Scope of this contribution is the characterization of the flow (velocities and layer thicknesses) on the dike crest in order to extend the theoretical models and provide criteria for the design of structures close to mean sea level or overwashed. This analysis is carried out on a numerical database obtained running the Rans-Vof code (IH-2VOF) developed by the University of Cantabria.
The paper structure is as follows. First the theoretical approach developed by Schuttrumpf and Oumeraci for emerged dikes is described in Section 2. Then the numerical model is briefly presented in Section 3. In Section 4 the numerical tests and its set-up are introduced. The key results obtained by the numerical simulation (for example the influence of the seaward-landward slope and of the dike submergence) are reported in Section 5. Then the analysis of the wave flow characteristics over the dike crest and the comparison with the theoretical approach are presented respectively in Sections 6 and 7. Finally, the capacity of the model to represent wave reflection is examined in Section 8. Conclusions are drawn in Section 9.

2. The theoretical approach

Schuttrumpf and Oumeraci (2005) derived and validated a set of theoretical formulas for the prediction of the layer thicknesses and the velocities of the overtopping flow on the seaward slope, the crest and the landward slope for emerged dikes. Therefore their empirical expressions represent the velocity and flow

[1]Dipartimento di Ingegneria Civile, Ambientale e dei Materiali "DICAM", University of Bologna, Viale del Risorgimento, Bologna 40136, Italy. andreanatalia.raosa2@unibo.it
[2]Dipartimento di Ingegneria Civile, Ambientale e dei Materiali "DICAM", University of Bologna, Viale del Risorgimento, Bologna 40136, Italy. barbara.zanuttugh@ unibo.it
[3]Environmental Hydraulics Institute "IH Cantabria", University of Cantabria, C/ Isabel Torres nº 15 Parque Científico y Tecnológico de Cantabria 39011, Santander, Spain, jav.lopez@unican.es

depths at the crest off-shore edge (u_A, h_A), at the crest inshore edge (u_B, h_B), and down the backside slope (u_{sb}, h_{sb}), as illustrated in Figure 1. The key parameters necessary for estimating the flow velocities and depths are the levee freeboard, R_c, the runup elevation exceeded by 2 percent of the waves, $Ru_{2\%}$, and a friction factor, f, that accounts for frictional energy loss as the overtopping wave travels across the levee crest and down the protected-side slope.

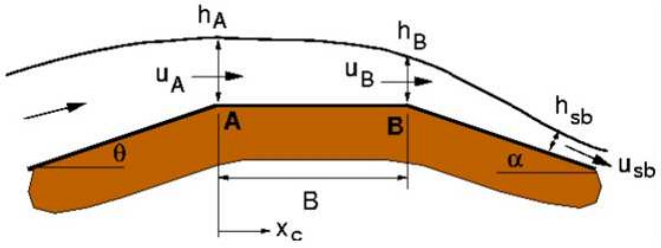

Figure 1. Wave overtopping definition sketch (Schütrumpf and Oumeraci, 2005).

2.1. *Overtopping flow depth on the dike crest*

The overtopping flow depth on the dike crest depends on the width of the crest B_c and the co-ordinate on the crest x_c. The decrease of the overtopping flow depth over the dike crest due to frictional losses and consequent overtopping volume deformation is described by the following exponential function:

$$\frac{h_c(x_c)}{h_c(x_c=0)} = \exp\left(-c_3 \frac{x_c}{x_B}\right) \tag{1}$$

where h_c is the overtopping flow depth on the dike crest, x_c=0 is the horizontal coordinate at the dike crest off-shore edge and c_3 is the dimensional coefficient equal to 0.75.

2.2. *Overtopping flow velocity on the dike crest*

A theoretical function for overtopping flow velocities on the dike crest has been developed by using the simplified Navier-Stokes-equations and the following assumptions: the dike crest is horizontal; the velocity components along the vertical to the dike slope can be neglected; the pressure term is almost constant over the dike crest; viscous effects in the flow direction are small; the bottom friction is constant over the dike crest. The following formula was verified by small and large scale model tests:

$$v_c = v_c(x_c=0)\cdot \exp\left(-\frac{x_c \cdot f}{2 \cdot h_c}\right) \tag{2}$$

where v_c is the overtopping flow velocity on the dike crest; v_c (x_c = 0) is the overtopping flow velocity at the beginning of the dike crest (x_c = 0); f is the friction coefficient.
From Equation 2 it can be derived that the overtopping flow velocity decreases along the dike crest due to bottom friction. The value of the friction factor f was determined to be *f=0.001* from model tests performed on straight and smooth slopes.

3. Description of the numerical model

Numerical models of fluid/wave-structure interactions are increasingly becoming a viable tool in furthering our understanding of the complicated phenomena that govern the hydraulic response of breakwaters, including effects of permeability (Losada, 2003). These include Lagrangian models with particle-based approaches such as the Moving Particle Semi-Implicit method (Koshizuka et al., 2005) and Smooth Particle Hydrodynamics (Dalrymple et al., 2009). For reasons ranging from computational efficiency to an accurate representation of the physical processes, Reynold Averaged Navier Stokes-Volume Of Fluid

(RANS-VOF) models such as those developed by Lara et al. (2008) and Shi et al. (2004) have become an attractive choice to model wave interactions with both solid as well as porous structures.
The RANS-VOF models noted above have been developed by implementing various extensions to the RIPPLE model (Kothe et al, 1991; originally designed to provide a solution of two-dimensional versions of the Navier-Stokes equations in a vertical plane with a free surface), making it specifically applicable to the study of wave interactions with coastal structures. The models solve the two-dimensional vertical (2DV) RANS equations and the k–ε equations for the turbulent kinetic energy (k), and the turbulent dissipation rate (ε). A non-linear algebraic Reynolds stress model is used to relate the Reynolds stress tensor and the strain rate of mean flow. The free surface movement is tracked by the Volume of Fluid (VOF) method. The flow inside the porous media is solved through the resolution of the Volume-Averaged Reynolds Averaged Navier–Stokes (VARANS) equations, which are derived by integrating the RANS equations over a control volume. In the VARANS equations, the interfacial forces between the fluid and solids are modeled according to the extended Forchheimer relationship, in which both linear and non-linear drag forces are included in the equations. An internal wavemaker based on a source function approach lends the models the ability to generate a wide range of desired wave conditions.
The models have undergone various validation procedures over the last decade or so, including wave interactions with low-crested structures (Losada et al., 2005), wave breaking on permeable slopes (Lara et al., 2006), surf zone hydrodynamics on natural beaches (Torres-Freyermuth et al., 2007), overtopping on rubble mound breakwaters and low-mound breakwaters including caissons on rubble mound foundations (Lara et al., 2008), and even ported caisson breakwaters (Shi et al. 2004). In this paper, we use the RANS-VOF model developed by Lara et al.. (2011) called IH-2VOF.

4. Description of the tests

Different simulations are performed in 1:10 scale in a numerical flume 52.3 m long and 1.5 m deep. The numerical wave paddle generates irregular waves with different significant wave heights *Hs* and peak period *Tp* (Table 1). For each wave attack the wave steepness remains constant and close to 2%. The dimensions of the structure (crest width and height) are constant while seaward and landward slopes are variable (Figure 2). Hence different tests for structures with different slopes (in-shore and off-shore) were carried out in order to study how the structure slopes affects the characteristics of the flow around the structure.
To understand the influence of the dike submergence on the evolution of the overtopping flow characteristics on the dike crest, tests with variable submergence were carried out by varying the water depth at the toe.
The following model settings are adopted:

- seaward boundary condition — *Hs* and *Tp* (Jonswap spectrum)
- landward boundary condition — absorption
- *k*-ε turbulence model
- flume dimension — 52.3 m x 1.5 m
- mesh resolution — cell width: 0.02÷0.05 m; cell height: 0.02 m
- mesh resolution on the dike crest — cell width: 0.02 m; cell height: 0.02 m

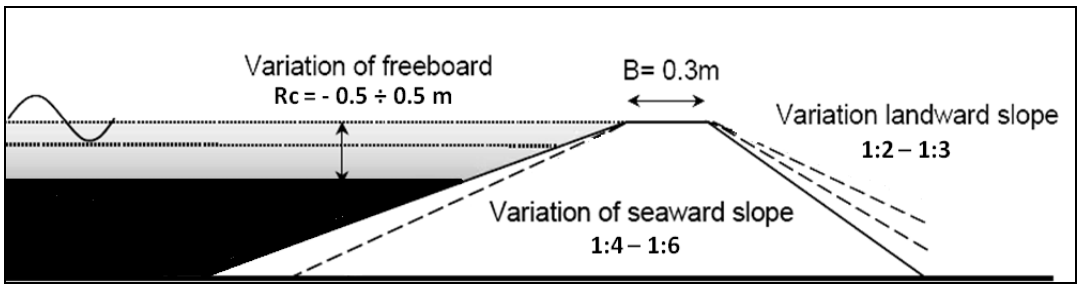

Figure 2. Tested levee cross section (model-scale units).

Table 1. Characteristics of simulated tests. R_c = freeboard (positive freeboard means submerged dike); *Hs* = significant wave height; *Tp* = peak period; *wd* = water depth; α_{off} = seaward slope; α_{in} = landward slope.

Cases	**α_{off} = 1:4 – α_{in} = 1:3**				**Cases**	**α_{off} = 1:4 – α_{in} = 1:2**				**Cases**	**α_{off} = 1:6 – α_{in} = 1:3**			
	Rc/Hs	**Hs (m)**	**Tp (s)**	**wd (m)**		**Rc/Hs**	**Hs (m)**	**Tp (s)**	**wd (m)**		**Rc/Hs**	**Hs (m)**	**Tp (s)**	**wd (m)**
T1A	1	1.00	5.5	8.00	**T1D**	1	1.00	5.5	8.00	**T1G**	1	1.00	5.5	8.00
T2A	1	1.00	6.9	8.00	**T2D**	1	1.00	6.9	8.00	**T2G**	1	1.00	6.9	8.00
T3A	1	2.00	10.4	9.00	**T3D**	1	2.00	10.4	9.00	**T3G**	1	2.00	10.4	9.00
T4A	1	2.00	13.8	9.00	**T4D**	1	2.00	13.8	9.00	**T4G**	1	2.00	13.8	9.00
T5B	0	1.00	5.5	7.00	**T5E**	0	1.00	5.5	7.00	**T5H**	0	1.00	5.5	7.00
T5B	0	1.00	6.9	7.00	**T5E**	0	1.00	6.9	7.00	**T5H**	0	1.00	6.9	7.00
T7B	0	2.00	10.4	7.00	**T7E**	0	2.00	10.4	7.00	**T7H**	0	2.00	10.4	7.00
T8B	0	2.00	13.8	7.00	**T8E**	0	2.00	13.8	7.00	**T8H**	0	2.00	13.8	7.00
T9C	1.5	1.00	5.5	8.50	**T9F**	1.5	1.00	5.5	8.50	**T9I**	1.5	1.00	5.5	8.50
T10C	1.5	1.00	6.9	8.50	**T10F**	1.5	1.00	6.9	8.50	**T10I**	1.5	1.00	6.9	8.50
T11C	1.5	2.00	10.4	10.00	**T11F**	1.5	2.00	10.4	10.00	**T11I**	1.5	2.00	10.4	10.00
T12C	1.5	2.00	13.8	10.00	**T12F**	1.5	2.00	13.8	10.00	**T12I**	1.5	2.00	13.8	10.00

5. Description of key results

The results obtained by the numerical analysis, i.e wave height and velocity development on the dike crest, are presented and compared with Schuttrumpf and Oumeraci's work. The values of $h_{2\%}$ and $u_{2\%}$ at the dike off-shore edge are summarized in Table 2 for all the tests. These values are compared with the following theoretical equations (Van der Meer et al., 2010):

$$h_{2\%}\left(x_c = 0\right) = c_{A,h}\left(R_{u2\%} - R_c\right) \tag{3}$$

$$u_{2\%}\left(x_c = 0\right) = c_{A,u}\sqrt{g\left(R_{u2\%} - R_c\right)} \tag{4}$$

where $h_{2\%}$ and $u_{2\%}$ are respectively the flow depth and velocity exceeded by 2% of the incident waves calculated numerically, $c_{A,h}$ is the coefficient for the flow depth and $c_{A,u}$ is the coefficient for the flow velocity. For the tests with R_c=0 the two coefficients are derived from Equations (3) and (4) and compared with the fitting of the empirical values proposed by Bosmann et al., (2008):

$$c_{A,h} = 0.01/\sin^2\alpha_{off}\,,\; c_{A,u} = 0.3/\sin\alpha_{off} \tag{5}$$

In Table 3 the numerical and theoretical coefficients are reported.
The following paragraphs investigate the effects of the structure design parameters (i.e. slopes and submergence) on the trend of both depths and velocities over the crest.

5.1 *Influence of the dike submergence*

Figure 3 shows on the left the wave height trend over the structure crest. In case of R_c=0, the evolution of the wave height is similar to that found by Schuttrumpf and Oumeraci and, more in general, by several authors in case of emerged structures (Bosman, 2008; Van Gent, 2002). By increasing the submergence, the decay is less marked and it completely disappears when R_c/Hs=1.5. The right panel of Figure 3 shows the evolution of the overtopping flow velocity. It can be observed that the velocity increases while the wave travels over the crest, and specifically the growth rate decreases with increasing dike submergence. Moreover, in the submerged cases, the decrease of flow depth and the increase of velocity start from about the middle of the crest of the structure and however are very modest.

5.2 *Influence of the seaward slope*

Figure 4 compares the evolution of the overtopping flow characteristics on the dike crest for the 1:4 (represented as void diamonds) and 1:6 seaward slopes (represented as crosses). It is possible to observe that, irrespectively of the submergence, the seaward slope does not significantly affect the evolution on the dike crest of the overtopping flow depth, to the left, and of the velocity, to the right. Only in case of R_c=0 (red color) a slight discrepancy among the velocity results obtained for different seaward slopes is present.

5.3 *Influence of the landward slope*

In Figure 5, the trends of the overtopping flow characteristics on the dike crest are reported for the structures with both landward slope 1:3 (represented as void diamonds) and 1:2 (represented as crosses). In the same graph the results obtained for different submergence are shown. As expected, the influence of the landward slope appears to be negligible. This means that the flow remains always subcritical over the crest under a sufficient hydraulic head.

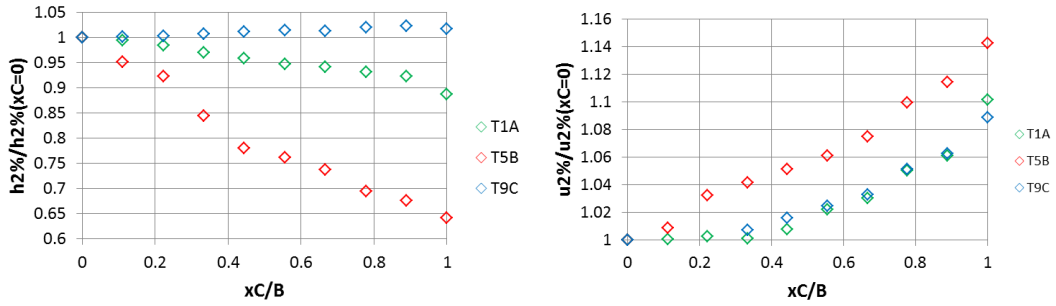

Figure 3. Wave height and velocity trend on the dike crest for test with R_c/Hs=1 (green), R_c/Hs=0 (red) and R_c/Hs=1.5 (blue).

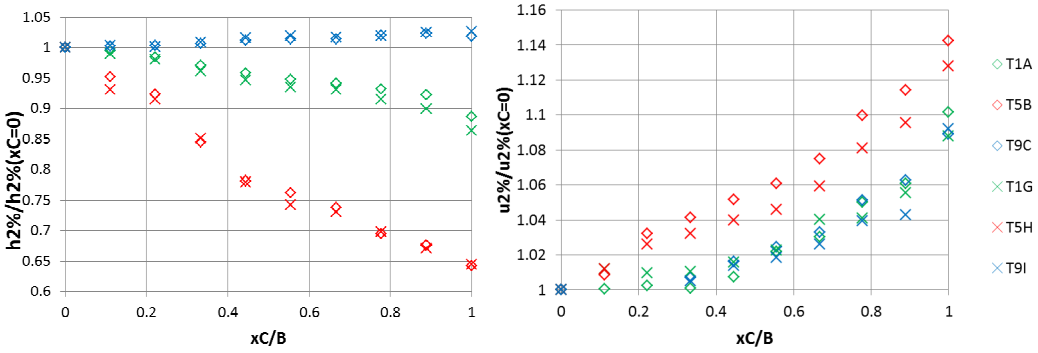

Figure 4. Wave height and velocity trend on the dike crest for tests characterized by seaward slope 1:4 (diamonds) and 1:6 (crosses) and different freeboard.

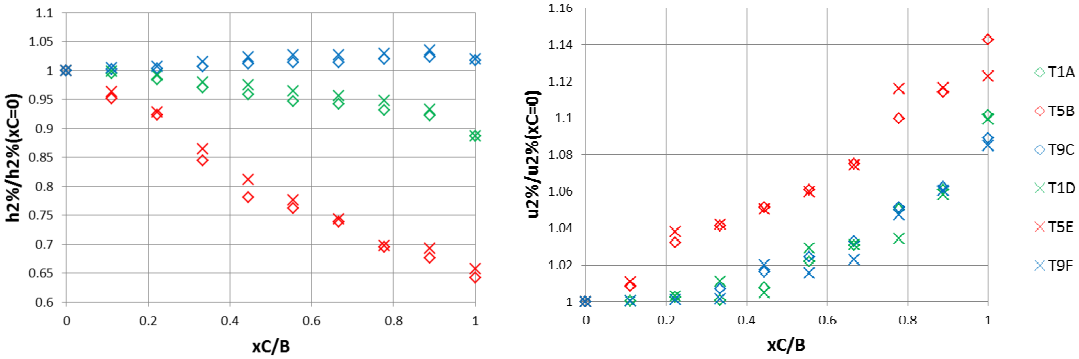

Figure 5. Wave height and velocity trend on the dike crest for tests characterized by landward slope 1:3 (diamonds) and 1:2 (crosses) and different freeboard.

Table 2. $h_{2\%}(x_c=0)$ = flow depth exceeded by 2% of the waves height at the off-shore edge; $u_{2\%}(x_c=0)$ = flow velocity exceeded by 2% of the waves height at the off-shore edge.

Tests	h2% (xc=0) (m)	u2% (xc=0) (m/s)	Tests	h2% (xc=0) (m)	u2% (xc=0) (m/s)	Tests	h2% (xc=0) (m)	u2% (xc=0) (m/s)
T1A	0.1170	0.3197	**T1D**	0.1199	0.3150	**T1G**	0.1180	0.3320
T2A	0.1484	0.3911	**T2D**	0.1524	0.3726	**T2G**	0.1179	0.3317
T3A	0.3070	0.6052	**T3D**	0.3009	0.6137	**T3G**	0.3089	0.6105
T4A	0.3041	0.6387	**T4D**	0.2977	0.6555	**T4G**	0.3107	0.6561
T5B	0.0550	0.6720	**T5E**	0.0549	0.6654	**T5H**	0.0497	0.6672
T6B	0.0682	0.7609	**T6E**	0.0688	0.7499	**T6H**	0.0624	0.7714
T7B	0.1446	1.1621	**T7E**	0.1445	1.1321	**T7H**	0.1170	1.2569
T8B	0.1698	1.1476	**T8E**	0.1672	1.1415	**T8H**	0.1523	1.2555
T9C	0.1123	0.2651	**T9F**	0.1167	0.2558	**T9I**	0.1134	0.2790
T10C	0.1440	0.3072	**T10F**	0.1502	0.2882	**T10I**	0.1469	0.3188
T11C	0.2912	0.4648	**T11F**	0.2844	0.4731	**T11I**	0.3024	0.4717
T12C	0.2782	0.5515	**T12F**	0.2685	0.5719	**T12I**	0.2896	0.5578

Table 3. $c_{A,h}$ =coefficient derived from Eq. 3; $c_{A,h}$ Bosmann= coefficient derived from Eq. 5 $c_{A,u}$ = coefficient derived by Eq. 4; $c_{A,u}$ Bosmann = coefficient derived from Eq. 5.

Tests	$c_{A,h}$	$c_{A,h}$ Bosmann	Tests	$c_{A,h}$	$c_{A,h}$ Bosmann	Tests	$c_{A,h}$	$c_{A,h}$ Bosmann
T5B	0.2050	0.1600	**T5E**	0.2044	0.1600	**T5H**	0.2777	0.3600
T6B	0.2345	0.1600	**T6E**	0.2368	0.1600	**T6H**	0.3011	0.3600
T7B	0.2602	0.1600	**T7E**	0.2601	0.1600	**T7H**	0.3158	0.3600
T8B	0.2899	0.1600	**T8E**	0.2855	0.1600	**T8H**	0.3534	0.3600
Tests	$c_{A,u}$	$c_{A,u}$ Bosmann	**Tests**	$c_{A,u}$	$c_{A,u}$ Bosmann	**Tests**	$c_{A,u}$	$c_{A,u}$ Bosmann
T5B	0.4143	1.2126	**T5E**	0.4102	1.2126	**T5H**	0.50374	1.8084
T6B	0.4508	1.2126	**T6E**	0.4443	1.2126	**T6H**	0.54154	1.8084
T7B	0.4980	1.2126	**T7E**	0.4852	1.2126	**T7H**	0.65974	1.8084
T8B	0.4790	1.2126	**T8E**	0.4765	1.2126	**T8H**	0.61104	1.8084

6. Analysis of wave flow characteristics over the dike crest

The purpose of this analysis is to fit the variation of the wave height/velocity over the dike crest by means of an appropriate curve and identify the key parameters of such fitting and their eventual dependence on structure and/or wave attack characteristics.

6.1 *Wave height evolution on the dike crest*

As well as in Schuttrumpf and Oumeraci's semi-empirical formulation, also these numerical results show that the overtopping wave height on the crest of the structure tends to decrease. Based on the numerical results, the decreasing curve is assumed to be a negative exponential, as in the semi-empirical formulation. In order to determine the decay coefficient, the best fitting curve and consequently the best fitting coefficient are identified for each test. These coefficients are reported in Tables 4 for both tests with R_c/Hs=0 and R_c/Hs=1. It is possible to observe that the coefficients depend on the wave height whereas they do not depend on the seaward slope. Four different average coefficients were therefore calculated for the two values of R_c/Hs and of Hs.

In Figure 6 the tests with R_c/Hs=0 and the curves obtained by the average coefficients of Table 4 are shown. In particular, the tests characterized by Hs=1 m and Hs=2 m are respectively reported in the left and right panels of the figure. The fitting curve provides an overall fair approximation, with greater discrepancy close to the inshore edge especially for the tests with Hs=2 m.

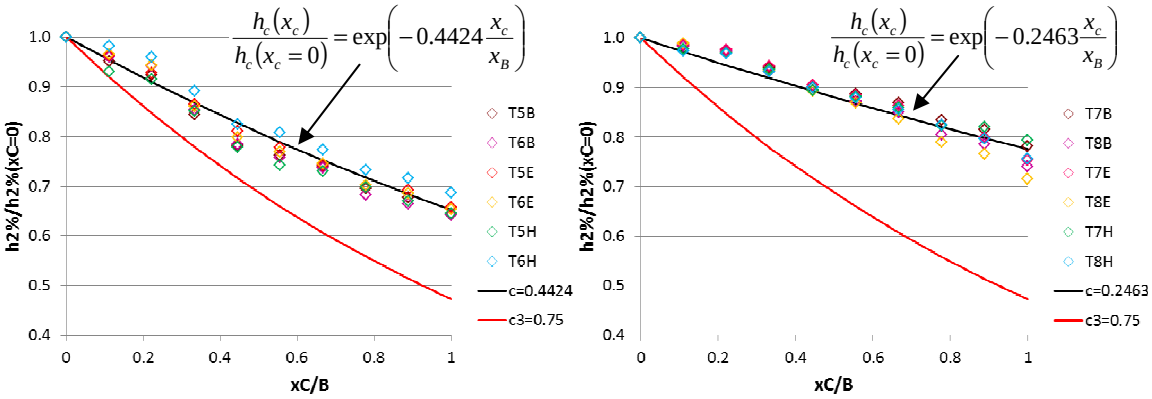

Figure 6. Wave height decay on the crest of the structure for tests with Hs=1m and R_c/Hs=0 on the left and with Hs=2m and R_c/Hs=0 on the right. Red curve shows the wave height decay obtained with Schuttrumpf and Oumeraci's coefficient (c_3=0.75).

Table 4. Coefficients obtained with the best fitting for the wave decay on the dike crest.

R_c/Hs=0	Hs=1 m	R_c/Hs=0	Hs=2 m	R_c/Hs=0	Hs=1 m	R_c/Hs=0	Hs=2 m
Tests	c_{best}	**Tests**	c_{best}	**Tests**	c_{best}	**Tests**	c_{best}
T5B	0.4557	**T7B**	0.2302	**T1A**	0.1511	**T3A**	0.0795
T6B	0.4595	**T8B**	0.2724	**T2A**	0.1806	**T4A**	0.0799
T5E	0.4463	**T7E**	0.2492	**T1D**	0.1692	**T3D**	0.0761
T6E	0.4409	**T8E**	0.2505	**T2D**	0.2181	**T4D**	0.0981
T5H	0.3905	**T7H**	0.2281	**T1G**	0.1196	**T3G**	0.0828
T6H	0.4616	**T8H**	0.2476	**T2G**	0.1117	**T4G**	0.0714
Average	0.4424	**Average**	0.2463	**Average**	0.1584	**Average**	0.0813

To understand the degree of approximation at the fitted formulation to the numerical data, the standard deviation for each test was calculated (see Table 5). The values of the standard deviation remains always under about 6% suggesting that the approximation is very good and in particular is more accurate for tests with Hs=1 m. Figure 7 shows the numerical results for tests with R_c/Hs=1 and the curves obtained by the average coefficients of Table 4. Tests with Hs =1 m and Hs =2 m on the left and on the right part of the figure are respectively reported. Also for these cases the same comments as to Figure 6 do apply: the quality of the fitting decreases (for both wave height) in the second half of the crest. By calculating the standard deviation for each test (see Table 5), it appears that the difference among computed and approximated values remains always under about 3%. Moreover, for tests with Hs=2 m the approximation is better and the standard deviation decreases of an order of magnitude.

Table 5. Standard deviation of wave decay on the dike crest.

R_c/Hs=0	σ'	R_c/Hs=0	σ'	R_c/Hs=1	σ'	R_c/Hs=1	σ'
T5B	2.09%	**T7B**	5.65%	**T1A**	1.57%	**T3A**	0.22%
T6B	2.43%	**T8B**	5.26%	**T2A**	1.93%	**T4A**	0.65%
T5E	1.19%	**T7E**	5.59%	**T1D**	2.65%	**T3D**	0.49%
T6E	1.67%	**T8E**	5.18%	**T2D**	2.81%	**T4D**	1.11%
T5H	2.51%	**T7H**	4.70%	**T1G**	1.74%	**T3G**	0.99%
T6H	2.68%	**T8H**	3.74%	**T2G**	1.98%	**T4G**	0.84%

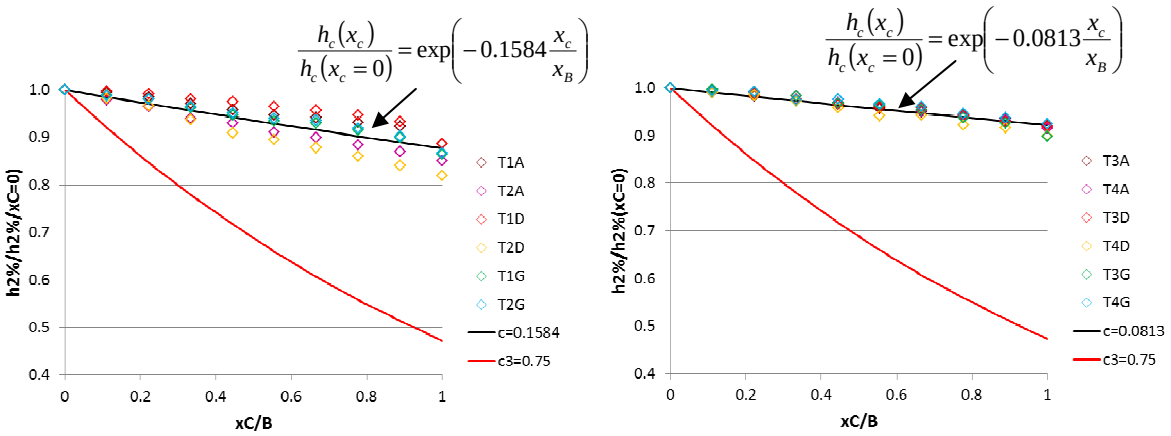

Figure 7. Wave height decay on the crest of the structure for tests with Hs=1m and R_c/Hs=0 on the left and with Hs=2m and R_c/Hs=0 on the right. Red curve shows the wave height decay obtained with Schuttrumpf and Oumeraci's coefficient (c_3=0.75).

6.2 *Wave velocity evolution on the dike crest*

The numerical tests show a slight increase of the velocity over the dike crest that can be approximated with a second-order polynomial function. The fitting coefficients for tests with R_c/Hs=0 and with R_c/Hs=1 are reported in Tables 6. Exactly as for the wave heights, also the coefficients of the velocity are found to be dependent on the wave height and not on the seaward slope.

In Figure 8 tests with R_c/Hs=0 and the polynomial function obtained by the average coefficients of Table 6 are shown. In particular, the tests characterized by Hs=1 m and Hs=2 m are respectively reported in the left and right panels of the figure. The trend of the velocity on the dike crest is very different for the tests with Hs=1 m and Hs=2 m. In the case of Hs=1 m the velocity tends to increase from the beginning of the crest, in the case of Hs=2 m there is a first phase of decrease and only after the middle of the crest width the velocity starts to increase.

The values of the standard deviation reported in Table 7 remains under about 1% showing that the approximation is always very good (irrespectively of the wave height).

Figure 9 compares the numerical results for tests with R_c/Hs=1 and the polynomial function obtained by the average coefficients of Table 6. Tests with Hs=1 m and Hs=2 m on the left and on the right part of the figure are respectively reported. Also in the submerged cases, the trend of the velocity on the dike crest is very different for the tests with different wave height. In particular a continuous velocity growth is found for the tests with Hs=1 m while for the tests with Hs= 2 m the velocity tends first to decrease and then to increase starting from the middle of the dike crest. By calculating the standard deviation for each test (see Table 7), it appears that the discrepancy from the curve remains always very low. In particular, the approximation is better for tests with Hs=1 m and the standard deviation remains always under 0.6%.

Table 6. Coefficients obtained with the best fitting for the tests with Rc/Hs=0.

Rc/Hs=1	Hs=1 m		Rc/Hs=1	Hs=1 m		Rc/Hs=1	Hs=1 m		Rc/Hs=1	Hs=1 m	
Tests	**a_{best}**	**b_{best}**	**Tests**	**a_{best}**	**b_{best}**	**Tests**	**a_{best}**	**b_{best}**	**Tests**	**a_{best}**	**b_{best}**
T5B	0.0525	0.0822	**T7B**	0.2604	0.1936	**T1A**	0.0794	0.0720	**T3A**	0.1736	0.1521
T6B	0.0776	0.0621	**T8B**	0.2518	0.1242	**T2A**	0.0563	0.0540	**T4A**	0.1878	0.1818
T5E	0.0644	0.0931	**T7E**	0.2541	0.1011	**T1D**	0.0261	0.0908	**T3D**	0.2364	0.1784
T6E	0.0844	0.0539	**T8E**	0.2435	0.1229	**T2D**	0.0446	0.1037	**T4D**	0.2842	0.1359
T5H	0.0617	0.0877	**T7G**	0.2515	0.1428	**T1G**	0.0365	0.0960	**T3G**	0.1844	0.1275
T6H	0.0806	0.0437	**T8G**	0.2572	0.1894	**T2G**	0.0330	0.0902	**T4G**	0.1966	0.1753
Average	0.0702	0.0845	**Average**	0.2105	0.1585	**Average**	=0.0459	0.0628	**Average**	0.1872	0.1218

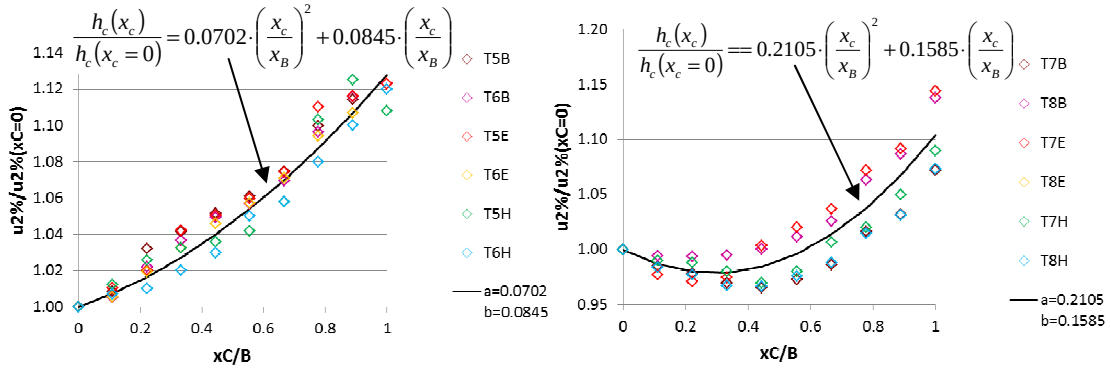

Figure 8. Wave velocity evolution on the crest of the structure for tests with *Hs*=1m and R_c/Hs=0 on the left and with *Hs*=2m and R_c/Hs=0 on the right.

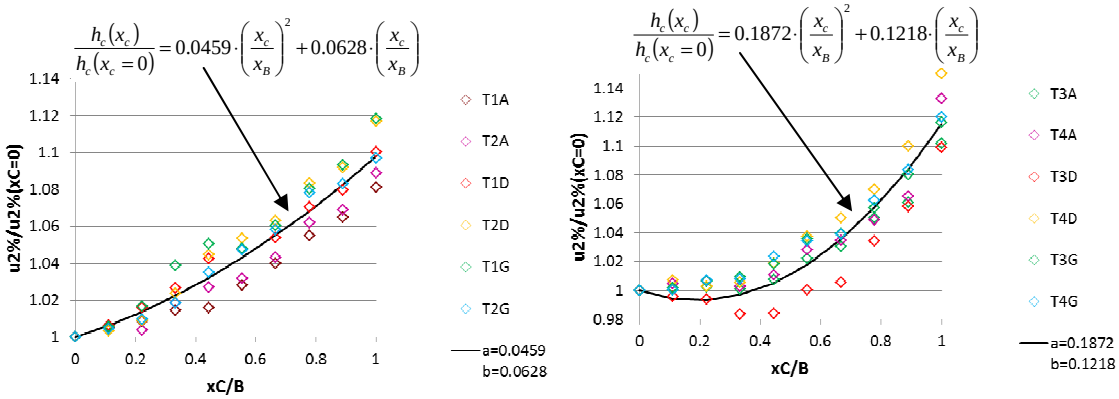

Figure 9. Wave velocity evolution on the crest of the structure for tests with *Hs*=1m and R_c/Hs=0 on the left and with *Hs*=2m and R_c/Hs=0 on the right.

Table 7. Standard deviation of the best fitting of the velocity change over the dike crest.

R_c/Hs=0	**σ'**	R_c/Hs=0	**σ'**	Rc/Hs=1	**σ'**	Rc/Hs=1	**σ'**
T5B	1.03%	**T7B**	0.02%	**T1A**	0.34%	**T3A**	1.26%
T6B	0.83%	**T8B**	0.02%	**T2A**	0.34%	**T4A**	0.89%
T5E	1.00%	**T7E**	0.02%	**T1D**	0.57%	**T3D**	0.42%
T6E	0.72%	**T8E**	0.03%	**T2D**	0.52%	**T4D**	1.02%
T5H	1.19%	**T7H**	0.02%	**T1G**	0.29%	**T3G**	1.16%
T6H	0.72%	**T8H**	0.03%	**T2G**	0.31%	**T4G**	0.41%

7. Verification of the discharge

Schüttrumpf (2001) and Schüttrumpf et al. (2001) provided equations for dimensionless average wave overtopping discharge based on laboratory experiments with *Rc*=0. Equations 6 and 7 from the Overtopping Manual (Pullen et al., 2007) are a slightly revised version of Schüttrumpf's equations:

$$\frac{q_w}{\sqrt{gH_{m0}^{\ 3}}} = 0.0537 \cdot \xi_{m-1,0} \qquad \text{for} \qquad \xi_{m-1,0} < 2 \tag{6}$$

$$\frac{q_w}{\sqrt{gH_{m0}^{\ 3}}} = \left(0.136 - \frac{0.226}{\xi_{m-1,0}}\right) \qquad \text{for} \qquad \xi_{m-1,0} \geq 2 \tag{7}$$

where $\xi_{m-1,0}$ is the Iribarren number based on deepwater wave length and mean energy wave period. Since the analysis deals with non-breaking waves, in this paper Equation 6 is adopted for comparison. The Overtopping Manual proposed to roughly calculate the combined wave and surge overtopping q_{ws} by superimposing the average wave overtopping discharge q_w estimated by Equations 6 or 7 with the steady surge overtopping q_s that would occur in the absence of waves, i.e.,

$$q_{ws} = q_w + q_s \tag{8}$$

where q_s is given by

$$q_s = 0.5443\sqrt{g}h_1^{3/2} \tag{9}$$

where h_1 is the upstream head (difference between surge elevation and levee crest elevation). Moreover, the suggestion of the Overtopping Manual to replace the coefficient a 0.5443 with 0.6 is followed.
Table 8 compares the theoretical q_{ws} and numerical values $q_{ws}NUM$. The discharge calculated numerically approximate very well the theoretical discharge, in fact, the error is between 1% and 12%. The error is calculated as

$$Er\% = \frac{q_{ws} - q_{ws}NUM}{q_{ws}} \cdot 100 \tag{10}$$

Table 8. Standard deviation for the tests with Rc/Hs=1 calculated theoretically q_{ws} and numerically $q_{ws}NUM$ and error calculated by Eq. 7.

Tests	**q_{ws}**	**q_{ws}NUM**	**Er%**	**Tests**	**qws**	**q_{ws}NUM**	**Er%**	**Tests**	**q_{ws}**	**q_{ws}NUM**	**Er%**
T1A	1.9831	1.9558	1.38	**T1D**	2.1575	2.9755	19.37	**T1G**	2.0644	1.9448	5.80
T2A	2.2029	2.3531	6.82	**T2D**	2.2029	2.3842	8.23	**T2G**	2.0947	1.9448	7.16
T3A	6.1595	6.2213	1.00	**T3D**	6.1595	6.2455	1.40	**T3G**	5.8772	6.2338	6.07
T4A	6.3006	6.6533	5.60	**T4D**	6.3006	6.6357	5.32	**T4G**	5.9713	6.6853	11.96
T5B	0.2736	0.4693	1.56	**T5E**	0.2736	0.3693	1.56	**T5H**	0.1824	0.2233	11.47
T6B	0.3164	0.2630	16.89	**T6E**	0.3164	0.2598	17.90	**T6H**	0.2109	0.2021	4.20
T7B	0.8005	0.5117	11.10	**T7E**	0.8005	0.5050	11.93	**T7H**	0.5337	0.6895	10.46
T8B	0.9312	0.8804	5.45	**T8E**	0.9312	0.8062	13.42	**T8H**	0.6208	0.6568	5.80
T9C	3.7323	3.9671	6.29	**T9F**	3.7323	3.9796	6.63	**T9I**	3.6384	3.9565	8.74
T10C	3.7789	3.3176	12.21	**T10F**	3.7789	3.3257	11.99	**T10I**	3.6695	3.3104	9.79
T11C	10.6265	10.2967	3.10	**T11F**	10.6265	10.3406	2.69	**T11I**	10.3377	10.2073	1.26
T12C	10.7724	10.1332	5.93	**T12F**	10.7724	10.1827	5.47	**T12I**	10.4349	9.9811	4.35

8. Considerations about wave reflection

The reflection coefficient obtained by the simulations is compared in Figure 10 with the data for smooth straight slopes that are included in the reflection database by Zanuttigh and Van der Meer (2006).
In this graph all the numerical tests for the structures with 1:4 and 1:6 seaward slopes are shown. These data are distributed along the vertical into two groups in correspondence of the two different values of ξ_0 depending on the slope.
The cases with R_c/Hs=0 (triangles) fall in the range of the experimental values for the tests with Hs=1m and above the experimental data for the tests with Hs=2m. The cases with R_c/Hs=1 (squares) and R_c/Hs=1.5 (diamonds) fall under the range of the experimental values for the tests with Hs=1m and in the experimental data for tests with Hs=2m.
The experimental data (Zanuttigh and Van der Meer, 2006) correspond to structures in design conditions (R_c/Hs<-0.5, emerged conditions): therefore all the numerical results were expected to fall below or within the database, whereas they appear indeed to be slightly greater than the experimental values. However, the numerical trends show two key issues in agreement with the physical process: the greater the submergence and/or the lower the wave height, the lower the reflection.

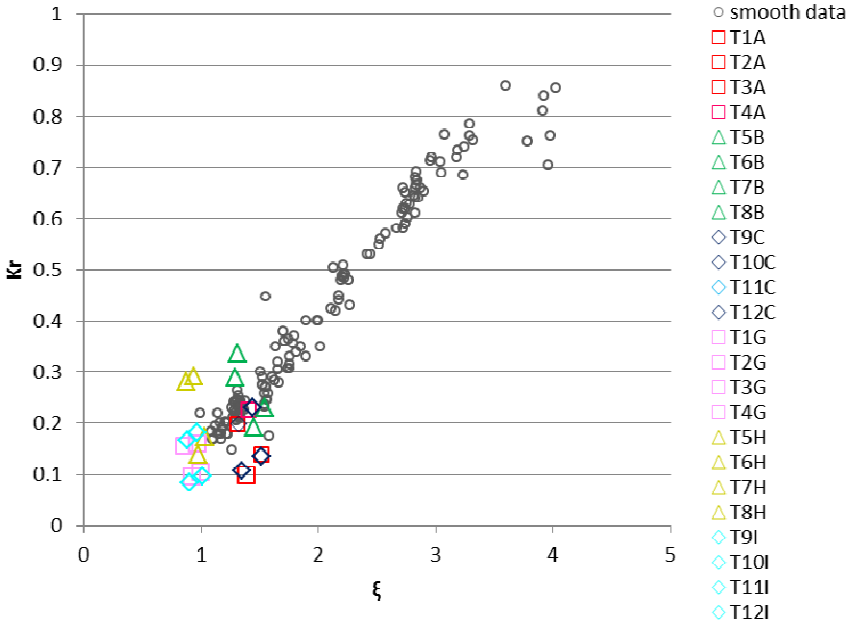

Figure 10. Wave reflection coefficient (*Kr*) obtained by the simulations and experimental database for smooth straight (Zanuttigh and Van der Meer, 2006).

9. Conclusions

Numerical simulations with the RansVof code (IH-2VOF model) developed by the University of Cantabria were carried out in order to analyze the flow characteristics (velocities and layer thicknesses) on the dike crest. The numerical data, derived by this analysis, allowed to perform a systematic investigation, which may be useful to extend the theoretical approach (Schuttrumpf and Oumeraci, 2005) and provide criteria for design application.
In the first part of the paper, the effects of the structure design parameters (i.e. slopes and submergence) on the trend of both depths and velocities over the crest are investigated.
As regards the influence of the submergence we can observe that:

- by increasing the submergence, the wave height decay is less marked and it completely disappears when Rc/Hs=1.5;
- the overtopping flow velocity increases while the wave travels over the crest; specifically its growth rate decreases by increasing the submergence;
- in the submerged cases, the decrease of flow depth and the increase of velocity start from about the middle of the crest of the structure and however are very modest.

As regards the influence of the seaward/landward slope:

- when the dike is submerged, the seaward slope does not significantly affect the evolution of the flow depth and velocity over the dike crest;
- only in case of R_c=0 the values of the flow depths over the crest appear to be affected by seaward slope;
- the results are independent from the landward slope.

In the second part of the paper, an appropriate curve able to fit the variation of the wave height/velocity over the dike crest and the key parameters of such fitting and their eventual dependence on structure and/or wave attack characteristics were found.

As regards the wave height:

- the numerical results show that the overtopping wave height on the dike crest tends to decrease as well as in Schuttrumpf and Oumeraci's work. Different decay coefficients were determined on the basis of the submergence and of the significant wave height.

As regards the wave velocity:

- the evolution of the velocity over the dike crest can be approximated with a second-order polynomial function and, as for the wave height, the fitting coefficients were found to be dependent on the wave height and submergence.

Finally, the discharge calculated numerically was compared with the theoretical formulas proposed by the Overtopping Manual. The approximation is very good, being the error between 1% and 12%.

Acknowledgments

The support of the European Commission through Contract 244104 THESEUS ("Innovative technologies for safer European coasts in a changing climate"), FP7.2009-1 Large Integrated Project, is gratefully acknowledged.

References

Bosman, G, J.W. Van der Meer, G. Hoffmans, H. Schüttrumpf and H.J. Verhagen. 2008. Individual overtopping events at dikes. ASCE, proc. *ICCE 2008*, Hamburg, Germany, p. 2944-2956.

EurOtop Manual. 2007. Wave Overtopping of Sea Defences and Related Structures – Assessment Manual. UK: W.H. Allsop, T. Pullen, T. Bruce. NL: J.W. van der Meer. DE: H. Schüttrumpf, A. Kortenhaus. www.overtopping-manual.com.

Lara, J.L., Losada, I.J., Liu, P.L.-F. 2006. Breaking waves over a mild gravel slope: experimental and numerical analysis. *Journal of Geophysical Research*, AGU, Vol. 111, C11019; doi: 10-1029/2005 JC003374.

Lara J.L., Losada I.J., R. Guanche. 2008. Wave interaction with low-mound breakwater using a rans model. *Ocean Engineering*, 56, 543-558.

Losada I.J. 2003. Advances in modeling the effects of permeable and reflective structures on waves and nearshore flows. In: Chris Lakhan, V. (Ed.), Advances in Coastal Modeling. *Elsevier Oceanography Series*, vol. 67.

Schüttrumpf, H.F.R. 2001. Wellenüberlaufströmung bei See-deichen, Ph.D.-thesis, Technical University Braunschweig.

Schuttrumpf H. and H. Oumeraci, 2005. Layer thicknesses and velocities of wave overtopping flow at sea dikes. *Journal of Coastal Engineering*, 52 (6), 473-495.

Shi F., Zhao Q., Kirby J.T., Lee D.S., S.N. Seo. 2004. Modeling wave interactions with complex coastal structures using an enhanced VOF model. In Proc. 29th *Int. Conf. Coastal Engineering*, Lisbon, 581-593.

Van der Meer, J.W., Bernardini, P., Snijders,W., Regeling, E., 2006. The wave overtopping simulator. *Proceedings of the 30th International Conference on Coastal Engineering*, vol. 5. World Scientific, 4654–4666.

Van der Meer J. W., B. Hardeman, G.J. Steendam, H. Schüttrumpf and H. Verheij, 2010. Flow depths and velocities at crest and landward slope of a dike, in theory and with the wave overtopping simulator. ASCE, Proc. *ICCE 2010*, Shanghai.

Van Gent M.R. 2002. Wave overtopping events at dikes. Proceedings of the 28th *International Coastal Engineering Conference*, vol. 2. World Scientific, 2203–2215.